Chemical Science

EDGE ARTICLE

View Article Online
View Journal | View Issue

Cite this: *Chem. Sci.*, 2014, **5**, 3309

Speciation and decomposition pathways of ruthenium catalysts used for selective C–H hydroxylation†

Cornelia Flender, Ashley M. Adams, Jennifer L. Roizen,‡ Eric McNeill, J. Du Bois* and Richard N. Zare*

Received 10th April 2014
Accepted 2nd June 2014

DOI: 10.1039/c4sc01050g

www.rsc.org/chemicalscience

Mechanistic insight into a C–H hydroxylation reaction catalysed by [(Me_3tacn)$RuCl_3$] has been obtained using desorption electrospray ionization mass spectrometry (DESI-MS) to identify reactive intermediates and to determine the fate of the starting metal complex. Our studies provide direct evidence for the formation of a high-valent dioxo-Ru(VI) species, which is believed to be the active oxidant. Other unexpected Ru-oxo intermediates, however, have been identified and may also function as competent hydroxylating agents. Mass spectral data that substantiate putative mechanisms for catalyst arrest and highlight reactivity differences between [(Me_3tacn)$RuCl_3$] and the corresponding tribromide adduct are also described.

Introduction

The hydroxylation of unactivated C–H bonds remains a leading challenge in modern organic chemistry despite recent, notable advances using both metal- and nonmetal-based catalysts to effect this transformation.[1,2,3,4] Following earlier work of Che, we have demonstrated the utility of (1,4,7-trimethyl-1,4,7-triazacyclononane)ruthenium(III) trichloride ([(Me_3tacn)$RuCl_3$], **1**) for oxidation of tertiary and certain benzylic C–H bonds on substrates of varying complexities (Fig. 1).[5] Under optimized conditions, the reaction is conducted in aqueous solution using either ceric ammonium nitrate (CAN) or sodium periodate ($NaIO_4$) as the stoichiometric oxidant. Mechanistic evidence, including both substrate selectivity and kinetic isotope effect data, suggest that oxidation occurs by an initial C–H abstraction event followed by fast, solvent-caged radical rebound. In order to gain additional insight into the reaction process and the mechanism(s) for catalyst arrest, we have utilized desorption electrospray ionization (DESI) coupled to mass spectrometry (MS)[6] to detect transient reaction intermediates and catalyst-derived products. These experiments have revealed three oxo-substituted Ru species, including the putative active oxidant, a dioxo-Ru(VI) Me_3tacn adduct; mono-oxo Ru(IV) and dioxo-Ru(V) adducts have also been identified by DESI-MS. Examination of MS data from spent reaction mixtures suggests possible mechanisms for inhibition of reaction turnover. Collectively, these results underscore the utility of DESI-MS as an analytical method for reaction methods development.[7]

Using DESI-MS, molecular ions corresponding to reaction intermediates with millisecond lifetimes can be detected.[8] The detection of such fleeting species is achieved by spraying charged droplets of a reagent with the assistance of a nebulizing gas onto a sample that is spotted on a surface (Fig. S1†). Upon impact of the reagent and the sample, secondary droplets that contain the reaction partners are desorbed from the surface and directed into the MS for analysis. The reaction is initiated at the time the reagent droplets hit the sample on the surface, and continues inside these secondary droplets. Evaporation of the droplets takes place inside the transfer capillary of the MS to give the desolvated ions. The close spatial proximity of the microdroplet source to the MS inlet capillary allows for very short mixing times.[9] In this study, we used DESI-MS to look at early time points of the [(Me_3tacn)$RuCl_3$]-catalysed C–H hydroxylation reaction. The distinct isotope profile of ruthenium and the high mass accuracy of an Orbitrap mass spectrometer[10] allow for accurate identification of reaction products.

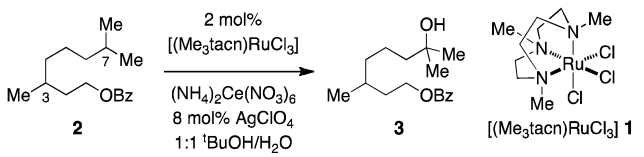

Fig. 1 Tertiary C–H bond hydroxylation under Ru-catalysis.

Department of Chemistry, Stanford University, Stanford, CA 94305, USA. E-mail: jdubois@stanford.edu; rnz@stanford.edu

† Electronic supplementary information (ESI) available. See DOI: 10.1039/c4sc01050g

‡ Present address: Department of Chemistry, Duke University 3236 French Science Center, 124 Science Drive Durham, NC 27708.

Results and discussion

A. High-valent Ru oxidants

The oxidation of tertiary and benzylic C–H bonds mediated by catalytic amounts of [(Me_3tacn)$RuCl_3$] **1** proceeds smoothly in an aqueous alcohol solvent mixture, and either tertiary alcohol or ketone products can be obtained in synthetically useful yields (45–82%). In general, CAN proves to be the most effective terminal oxidant for this transformation.[11] The addition of a chloride scavenger, $AgClO_4$, improves turnover number and overall product yields. The Ag(I) source is presumed to dissociate the Cl^- groups from the [(Me_3tacn)$RuCl_3$] complex prior to the addition of oxidant. Initial DESI-MS studies, therefore, began by assessing the efficiency of this pre-incubation procedure. Catalyst **1** was treated with 4 equiv. of $AgClO_4$, the solution filtered and spotted on a paper surface for DESI analysis (Fig. 2, top). In the mass spectrum, the most abundant signal corresponds to a molecular formula $[LRuO_2H_3Cl]^+$ (L = Me_3tacn). This finding demonstrates that the removal of a three chloride ligands by $AgClO_4$ is not complete prior to the addition of oxidant.

Our initial finding from DESI-MS that $AgClO_4$ does not affect complete dissociation of chloride ligands prompted us to synthesize the corresponding tribromide complex, [(Me_3tacn)$RuBr_3$]. Analysis of this catalyst prior to treatment with Ag(I) reveals three major forms, $[LRuOBr_2H]^+$, $[LRuO_2BrH_2]^+$ and $[LRuO_3H_3]^+$ with $[LRuO_2BrH_2]^+$ as the primary component (Fig. S2†). This finding contrasts analogous data with [(Me_3tacn)$RuCl_3$], a complex that exists in solution almost exclusively as the tris-chloride adduct (Fig. S3).† DESI analysis of [(Me_3tacn)$RuBr_3$] following treatment with $AgClO_4$ shows $[LRuO_3H_4]^+$ as the only Ru-containing species in the spectrum (Fig. 2, bottom). From these data, it is evident that the bromide ligand is considerably more labile that its chloride counterpart.

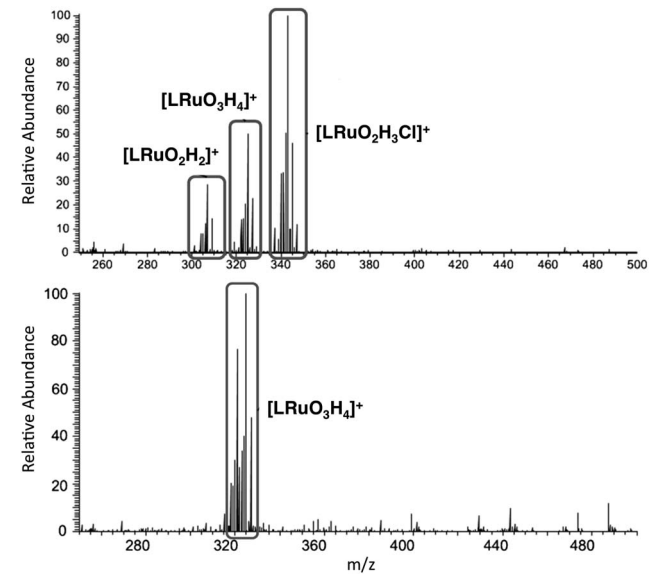

Fig. 2 DESI spectra of [(Me_3tacn)$RuCl_3$] (top) and [(Me_3tacn)$RuBr_3$] (bottom) both incubated with $AgClO_4$.

DESI-MS of the reaction of [(Me_3tacn)$RuCl_3$] with substrate **2** and $NaIO_4$ shows a cationic ruthenium(VI) complex as the major Ru-containing analyte, which we have assigned as $[LRuO_2(OH)]^+$ **4** (Fig. 3). Detection of this dioxo-Ru(VI) species is consistent with the mechanism of Che and co-workers that a dioxo-adduct is the active hydroxylating agent.[12] In addition to **4**, we were able to identify a second dioxo complex, $[LRuO_2]^+$ **5** (Fig. 3). Subjecting $[LRuO_2]^+$ **5** to collision induced dissociation (CID) requires a relative collision energy of 20% to fragment the ligand. Subjecting $[LRuO_2(OH)]^+$ to CID, however, leads to loss of H_2O at a relative energy of 10%, which can be attributed to loss of the OH-group and fragmentation of the ligand. Further experiments without the application of external voltage demonstrated that the composition of the spectrum did not change; applying a 5 kV potential to the syringe supplying the spray resulted in increased overall signal intensity.[13] To determine the origin of the oxo-groups, ^{18}O-labelled H_2O was employed as solvent. Corresponding mass shifts of 6 Da for $[LRuO_2(OH)]^+$ **4** and 4 Da for $[LRuO_2]^+$ **5** were recorded. These data confirm that the oxygen ligands present in these ions either originate from or are rapidly exchanged with solvent under these conditions.[14]

Upon further analysis of the signal corresponding to $[LRuO_2]^+$ **5**, a third ruthenium-containing species was identified with a $\Delta m/z$ of +1 Da. While this peak is low intensity, it is well resolved by the Orbitrap MS (set to 60 000 at m/z 400). This new species has one additional hydrogen compared to $[LRuO_2]^+$ and has been assigned as a mixed hydroxy-oxo-Ru(IV) adduct **6**

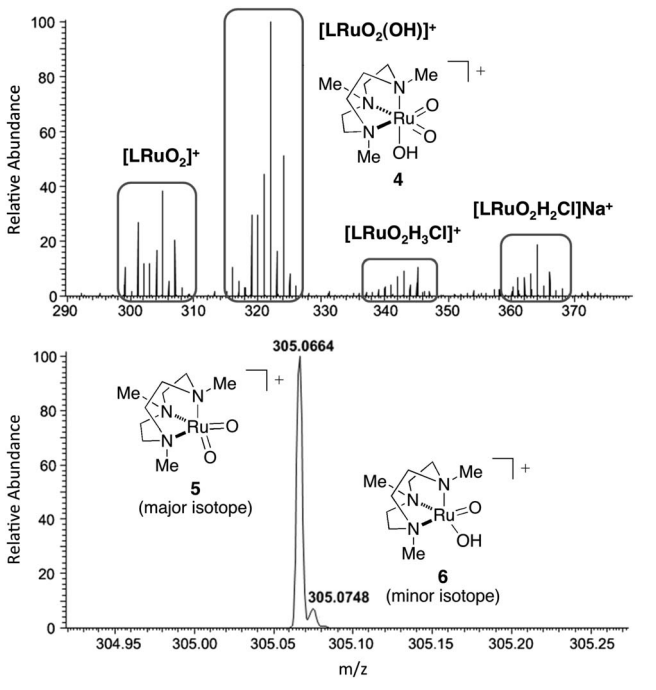

Fig. 3 Top: DESI mass spectrum of [(Me_3tacn)$RuCl_3$], pre-treated with $AgClO_4$, and substrate **2** sprayed with $NaIO_4$. For full spectrum see Fig. S4.† Bottom: zoom-in of the signal corresponding to $[LRuO_2]^+$ and proposed structures for both metal-oxo species. The main isotope of $[LRuO(OH)]^+$ **6** is at m/z 306.0755.

(Fig. 3, bottom). To verify this result, experiments were repeated using different types of surfaces to spot the sample (paper, glass or PTFE), with and without the application of voltage. Signals corresponding to **5** and **6** appear in the spectrum irrespective the experimental conditions. Analogous data were recorded when [(Me_3tacn)$RuBr_3$] was used in place of **1** (Fig. S5†). While the formation of a mono-oxo Ru(IV) was unexpected, complexes of this type have been previously characterized.[15] In one example, Che has described the synthesis of a (Me_3tacn)(bipyridine)Ru(IV)-oxo species, which is capable of oxidizing benzylic and aromatic C–H bonds.[16] Our DESI-MS experiments establish that the combination of [(Me_3tacn)-$RuCl_3$], $AgClO_4$, and $NaIO_4$ is capable of generating at least three discrete oxidized ruthenium intermediates. While it is possible that the dioxo-Ru(VI) adduct **4** functions as the reactive hydroxylating agent, substrate oxidation by Ru(V) **5** and/or Ru(IV) **6** species cannot be discounted at this time.

Due to the nature and number of oxidized ruthenium adducts detected in the DESI-MS spectra, we were interested in examining the relationship between oxidant concentration and catalyst speciation. Varying concentrations of $NaIO_4$ were sprayed onto a mixture of [(Me_3tacn)$RuCl_3$], pre-incubated with $AgClO_4$, and substrate **2**. Fig. 4 shows that the intensity of the Ru(III) species [(Me_3tacn)RuO_3H_4]$^+$ decreases with increasing concentrations of oxidant. Both **5** and **6** show a maximum intensity at higher oxidant concentrations. The maximum signal for **6** is recorded at [$NaIO_4$] of 10^{-5} M. By contrast, **5** has a signal maximum at an oxidant concentration of 10^{-4} M. These results suggest that conversion of **6** to **5** may be occurring at higher periodate concentrations. Above 10^{-4} M [$NaIO_4$], the principal ruthenium species are in the dioxo form (*i.e.*, **4** and **5**).

B. Catalytic turnover and catalyst arrest

Our inability to improve yields of C–H hydroxylation products by increasing [(Me_3tacn)$RuCl_3$] loading has prompted experiments to understand mechanisms for catalyst arrest.[17] The formation of oxo-bridged diruthenium species may be one pathway for catalyst inactivation.[18] We have performed DESI-MS analysis of reaction mixtures following a 24 h mixing period of catalyst **1**, substrate **2**, $AgClO_4$, and $NaIO_4$. The reaction mixture was partitioned between aqueous and ethereal solvents, and the contents of each fraction were analysed separately. The full spectrum of the aqueous extract shows the complex composition of the spent mixture (Fig. 5).

Analysing the signals that contain at least one ruthenium ion, we have found that all such compounds are in the mass range of 250–650 *m*/*z*. After 24 hours, no oxo- or dioxo-derived species can be identified. Notably, these experiments reveal a trioxo-bridged ruthenium dimer, [(Me_3tacn)RuO_3Ru(Me_3tacn)]$^{2+}$ **7**, which is detected as a doubly charged species (Fig. 5). We believe that dimer formation represents at least one of multiple pathways for inhibition of catalyst turnover. Accordingly, when a solution of $NaIO_4$ (5×10^{-4} M) was sprayed onto a sample of the spent reaction mixture, the MS spectrum did not show any increase in the intensity of hydroxylation products (Fig. S6†). These results suggest that the ruthenium species present at the end of the reaction, which includes dimer **7**, are no longer active as C–H hydroxylation catalysts. A full list of identified *m*/*z* signals, including a variety of mononuclear ruthenium species, is given in Fig. S7 and S8.† The [(Me_3tacn)$RuBr_3$] yields similar decomposition products as the [(Me_3tacn)$RuCl_3$] catalyst (see Fig. S9†), including the trioxo-bridged dimer.

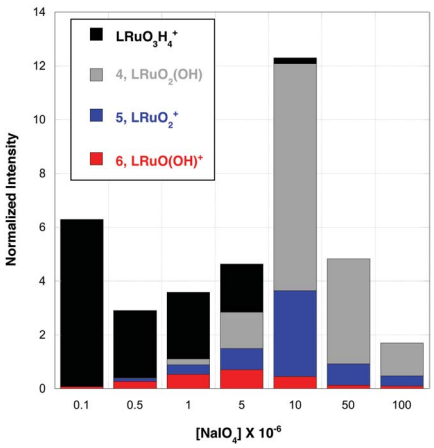

Fig. 4 Ruthenium speciation at varying $NaIO_4$ concentrations. Ion intensities were normalized to the total ion count (TIC) of all ruthenium containing species.

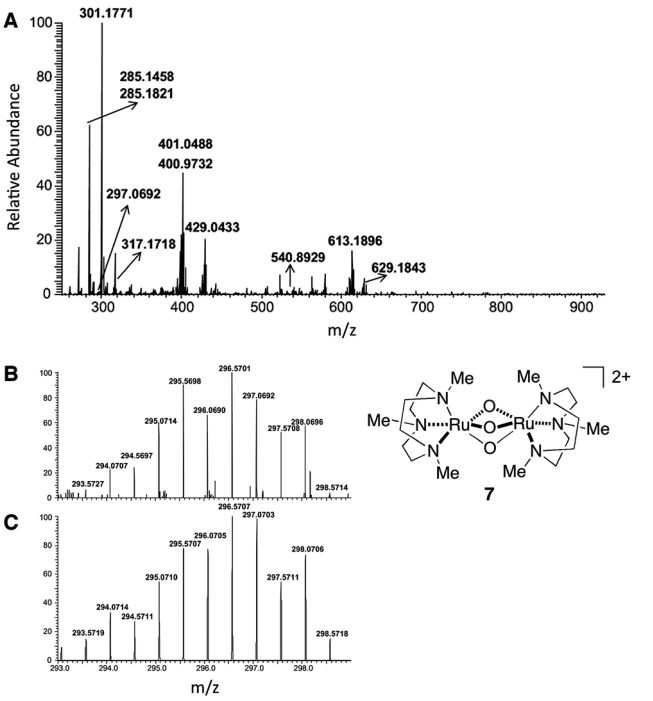

Fig. 5 (A) DESI-mass spectrum of the aqueous fraction following work-up of a spent reaction mixture (catalyst **1**, $AgClO_4$, **2**, and $NaIO_4$, 24 h). (B) Experimental spectrum showing an isotope profile consistent with trioxo-bridged ruthenium dimer **7**. (C) Simulated spectrum of **7** (note: 0.5 *m*/*z* intervals between isotopes are consistent with the assignment of a dimer having a net dipositive charge).

Mass spectral analysis of the ethereal extract of the spent mixture from a reaction with [(Me$_3$tacn)RuCl$_3$] is shown in Fig. S10.† In addition to the major product **3**, five byproducts derived from **2** can be identified (Table 1). These include the bis-diol product **3a** resulting from hydroxylation at both tertiary sites (*i.e.*, C3 and C7) as well as two ketone products that stem from oxidation at any one of the four unsubstituted methylene centers (**3b** and **3c**). Two additional products, **3d** and **3e**, arise from oxidative C–C bond cleavage (possibly through an alkene intermediate). To confirm the chemical formula assignments of the reaction products, a d$_5$-benzoate-labeled substrate was synthesized. Oxidation of this compound leads to a 5 Da mass shift for the mono-hydroxylated product and all other substrate-derived byproducts (Fig. S10†). Finally, examination of the product distribution over time (Table 2) shows that the reaction is effectively complete at 3 hours. These data also demonstrate that, as the reaction proceeds, the ruthenium trioxo-ruthenium dimer **7** is formed.

In bulk solution, [(Me$_3$tacn)RuBr$_3$] is less effective than [(Me$_3$tacn)RuCl$_3$] as a pre-catalyst for C–H hydroxylation of **1**, and affords only 20% of **3** at 2 mol% loading. When the reaction with [(Me$_3$tacn)RuBr$_3$] is examined by DESI-MS (24 h), the signal corresponding to substrate **2** (*m*/*z* 285.18) is significantly more intense than that of the product **3** (*m*/*z* 301.17, Fig. 6a). This finding is consistent with the bulk solution data, and contrasts rather markedly the reaction with [(Me$_3$tacn)RuCl$_3$]. The kinetic profile of the reaction progress, as assessed by DESI-MS, demonstrates the superiority of the [(Me$_3$tacn)RuCl$_3$] catalyst

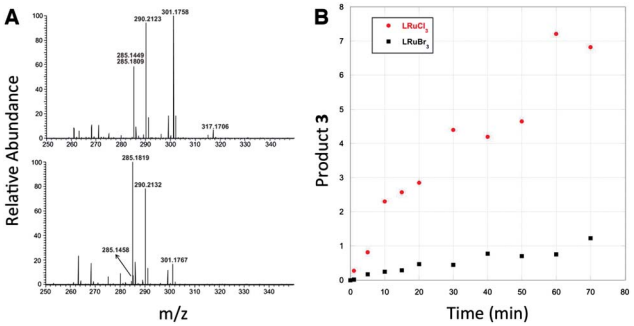

Fig. 6 (A) Incubated reaction mixtures of (top) [(Me$_3$tacn)RuCl$_3$] *versus* (bottom) (Me$_3$tacn)RuBr$_3$. The signals at *m*/*z* 301.17, 317.17, 285.18, and 285.14 correspond to the following products: alcohol **3**, diol **3a**, substrate **2**, ketone **3b** or **c**, respectively. The signal at *m*/*z* 290.21 is an internal standard. (B) A plot of product **3** formation *vs.* time for a reaction catalysed by [(Me$_3$tacn)RuCl$_3$] (red) and [(Me$_3$tacn)RuBr$_3$] (black).

Table 1 Major and minor byproducts from C–H hydroxylation catalysed by **1**. Structures shown for compounds **3b** and **3c** are representative isomers and have not been definitively assigned. Compounds **3d** and **3e** are products arising from C–C bond cleavage

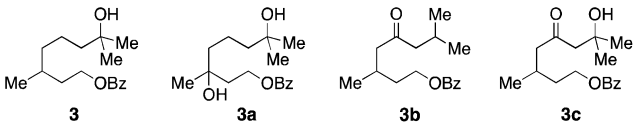

Entry	Sum formula	*m*/*z*	Relative signal intensity
3	$[C_{17}H_{26}O_3]Na^+$	301.1774	100%
3a	$[C_{17}H_{26}O_4]Na^+$	317.1723	4.5%
3b	$[C_{17}H_{24}O_3]Na^+$	299.1618	17.5%
3c	$[C_{17}H_{24}O_4]Na^+$	315.1567	2.5%
3d	$[C_{16}H_{22}O_3]Na^+$	285.1461	10.5%
3e	$[C_{16}H_{20}O_4]Na^+$	299.1254	3.0%

Table 2 Changes in the signal intensities (normalized) *vs.* time of selected ions

Time (h)	Substrate **2**	Product **3**	Dimer **7**
0.15	162	7	0
0.5	68	43	0
3	55	106	1.72
24	57	108	1.65

(Fig. 6b). In spite of the presence of Ag(I), the effect of the counterion (Cl *vs.* Br) on both the speciation of the catalyst and its performance is clear.

Conclusions

Our studies have focused on the identification of the active oxidants and potential arrest mechanisms in the [(Me$_3$tacn)-RuCl$_3$]-catalysed hydroxylation of tertiary C–H bonds. Comparative experiments with [(Me$_3$tacn)RuBr$_3$] have also been conducted, and reveal striking differences between these two catalysts, which is reflected in their disparate performance in solution. The power of DESI-MS to detect reaction intermediates and products within milliseconds following initiation is a considerable advantage of this analytical technique. Data from these experiments have raised unforeseen questions regarding the structure(s) of the active oxidant in this Ru-catalysed process. Future efforts to develop next-generation Ru systems for C–H hydroxylation may consider ligand designs that bias generation of a single oxidizing species. In addition to these findings, DESI-MS data has given evidence that catalyst dimerization, in this case to form a trioxo-bridged complex, is deleterious to catalyst turnover. The design of alternative ligand–metal complexes and/or discovery of reaction conditions that mitigate these second order processes could result in a significant boost in reaction performance.

Experimental section

The synthesis of the ligand Me$_3$tacn (1,4,7-trimethyl-1,4,7-triazacyclo-nonane) is described in detail elsewhere.[19] [(Me$_3$tacnRu)Cl$_3$] was obtained by metalation of 40 μL Me$_3$tacn with 199 mg [RuCl$_2$(dmso)$_4$] in 1.0 mL ethanol followed by refluxing in concentrated HCl.[20] [(Me$_3$tacn)RuBr$_3$] was synthesized accordingly using RuCl$_2$(dmso)$_4$ as the starting material and refluxing in HBr. Activation of the catalyst was carried out by dissolving 2 mg the Ru complex in 0.5 mL H$_2$O and sonicating until fully dissolved. 5 mg AgClO$_4$ (Sigma-Aldrich) was added and the

mixture stirred at 80 °C for 6 min. The heterogeneous mixture was cooled to room temperature, filtered through a cotton plug, and the mass analysed. For the analysis of incubated reaction mixtures, the suspension was transferred into a vial containing 37 mg substrate **2** and 85 mg $NaIO_4$. The contents were stirred for a prescribed amount of time (10 min, 30 min, 3 h, 24 h), then filtered through a cotton plug. The aqueous fraction was extracted with 3 × 1 mL of Et_2O. DESI-MS experiments were carried out using a homebuilt DESI source (described in S1†) coupled to an LTQ-XL Orbitrap mass spectrometer (Thermo Scientific). The instrument parameters were set as follows: temperature inlet capillary: 200 °C; resolution: 60 000 at *m*/*z* 400; scan range: 50–1000 *m*/*z*; voltage applied to syringe: 5 kV.

Acknowledgements

We gratefully acknowledge financial support from the National Science Foundation under the CCI Center for Selective C–H Functionalization (CHE-1205646). We would like to thank Jialing Zhang for help with DESI-MS experiments. J.L.R. was supported as a Ruth Kirschstein NIH postdoctoral fellow (5F32GM089033). C.F. and J.L.R thank the Center for Molecular Analysis and Design at Stanford University (CMAD) for postdoctoral fellowship support.

Notes and references

1 For general reviews on C–H hydroxylation, see: (*a*) T. Newhouse and P. B. Baran, *Angew. Chem., Int. Ed.*, 2011, **50**, 3362–3374; (*b*) M. C. White, *Science*, 2012, **335**, 807–809; (*c*) V. S. Thirunavukkasrasu, S. I. Kozhushkov and L. Ackerman, *Chem. Commun.*, 2014, **50**, 29–39; (*d*) A. Company, J. Lloret, L. Gomez and M. Costas, *Alkane C–H Activation by Single-Site Metal Catalysis*, Springer, Netherlands.

2 For examples of non-metal catalysed C–H hydroxylation, see: (*a*) B. H. Brodsky and J. Du Bois, *J. Am. Chem. Soc.*, 2005, **127**, 15391–15393; (*b*) N. D. Litvinas, B. H. Brodsky and J. Du Bois, *Angew. Chem., Int. Ed.*, 2009, **48**, 4513–4516; (*c*) A. M. Adams and J. Du Bois, *Chem. Sci.*, 2014, **5**, 656–659.

3 For examples with stoichiometric oxidants, see: (*a*) R. Curci, L. D'Accolti and C. Fusco, *Acc. Chem. Res.*, 2006, **39**, 1–9 and references therein; (*b*) K. Chen, J. M. Richter and P. S. Baran, *J. Am. Chem. Soc.*, 2008, **130**, 7247–7249; (*c*) K. Chen and P. S. Baran, *Nature*, 2009, **459**, 824–828.

4 For recent examples of transition-metal catalysed C–H hydroxylations, see: (*a*) C. Kim, K. Chen, J. Kim and L. Que Jr., *J. Am. Chem. Soc.*, 1997, **119**, 5964–5965; (*b*) S. Lee and P. L. Fuchs, *J. Am. Chem. Soc.*, 2002, **124**, 13978–13979; (*c*) M. S. Chen and M. C. White, *J. Am. Chem. Soc.*, 2004, **126**, 1346–1347; (*d*) S. Lee and P. L. Fuchs, *Org. Lett.*, 2004, **6**, 1437–1440; (*e*) A. R. Dick, K. L. Hull and M. S. Sanford, *J. Am. Chem. Soc.*, 2004, **126**, 2300–2301; (*f*) M. S. Chen and M. C. White, *Science*, 2007, **318**, 783–787; (*g*) A. Company, L. Gomez, X. Fontrodona, X. Ribas and M. Costas, *Chem.–Eur. J.*, 2008, **14**, 5727–5731; (*h*) N. A. Vermeulen, M. S. Chen and M. C. White, *Tetrahedron*, 2009, **65**, 3078–3084; (*i*) Y.-H. Zhang and J.-Q. Yu, *J. Am. Chem. Soc.*, 2009, **131**, 14654–14655; (*j*) M. S. Chen and M. C. White, *Science*, 2010, **327**, 566–571; (*k*) A. Company, I. Prat, J. R. Frisch, R. Mas-Balleste, M. Guell, G. Juhasz, X. Ribas, E. Munck, J. M. Luis, L. Que Jr. and M. Costas, *Chem.–Eur. J.*, 2011, **17**, 1622–1634; (*l*) I. Prat, J. S. Mathieson, M. Guell, X. Ribas, J. M. Luis, L. Cronin and M. Costas, *Nat. Chem.*, 2011, **3**, 788–793; (*m*) E. McNeill and J. Du Bois, *J. Am. Chem. Soc.*, 2010, **132**, 10202–10204.

5 E. McNeill and J. Du Bois, *Chem. Sci.*, 2012, **3**, 1810–1813.

6 (*a*) Z. Takáts, J. M. Wiseman, B. Gologan and R. G. Cooks, *Science*, 2004, **306**, 471–473; (*b*) Z. Takáts, J. M. Wiseman and R. G. Cooks, *J. Mass Spectrom.*, 2005, **40**, 1261–1275.

7 (*a*) K. L. Vikse, Z. Ahmadi, C. C. Manning, D. A. Harrington and J. S. McIndoe, *Angew. Chem., Int. Ed.*, 2011, **50**, 8304–8306; (*b*) F. Coelho and M. N. Eberlin, *Angew. Chem., Int. Ed.*, 2011, **50**, 5261–5263; (*c*) L. Zhu, G. Gamez, H. W. Chen, H. X. Huang, K. Chingin and R. Zenobi, *Rapid Commun. Mass Spectrom.*, 2008, **22**, 2993–2998; (*d*) A. J. Ingram, D. Solis-Ibarra, R. N. Zare and R. H. Waymouth, *Angew. Chem., Int. Ed.*, 2014, **53**, 5648–5652.

8 (*a*) J. R. Johansson and B. Norden, *Proc. Natl. Acad. Sci. U. S. A.*, 2012, **109**, 2186–2187; (*b*) R. H. Perry, K. R. Brownell, K. Chingin, T. J. Cahill, R. M. Waymouth and R. N. Zare, *Proc. Natl. Acad. Sci. U. S. A.*, 2012, **109**, 2246–2250; (*c*) R. H. Perry, T. J. Cahill, J. L. Roizen, J. Du Bois and R. N. Zare, *Proc. Natl. Acad. Sci. U. S. A.*, 2012, **109**, 18295–18299; (*d*) E. Gouré, F. Avenier, P. Dubourdeaux, O. Sénèque, F. Albrieux, C. Lebrun, M. Clémancey, P. Maldivi and J.-M. Latour, *Angew. Chem., Int. Ed.*, 2014, **53**, 1580–1584.

9 R. H. Perry, M. Splendore, A. Chien, N. K. Davis and R. N. Zare, *Angew. Chem., Int. Ed.*, 2011, **50**, 250–254.

10 R. H. Perry, R. G. Cooks and R. J. Noll, *Mass Spectrom. Rev.*, 2008, **27**, 661–699.

11 DESI-MS spectra were analogous for experiments performed with either ceric ammonium nitrate (CAN) or $NaIO_4$. $NaIO_4$ showed reduced ion suppression at higher concentrations and was therefore preferred for these studies.

12 (*a*) S. L. F. Chan, Y. H. Kan, K. L. Yip, J. S. Huang and C.-M. Che, *Coord. Chem. Rev.*, 2011, **255**, 899–919; (*b*) W. C. Cheng, W. Y. Yu, K. K. Cheung and C.-M. Che, *J. Chem. Soc., Chem. Commun.*, 1994, 1063–1064.

13 These data rule out the possibility that oxo-adducts originate from the electrospray process, see: S. P. Pasilis, V. Kertesz and G. Van Berkel, *J. Anal. Chem.*, 2008, **80**, 1208–1214. In addition, no Ru-oxo species are detected when experiments are performed in the absence of $NaIO_4$.

14 For examples of H_2O^{18} exchange with Ru-oxo species, see: C. Wang, K. V. Shalyaev, M. Bonchio, T. Carofiglio and J. T. Groves, *Inorg. Chem.*, 2006, **45**, 4769–4782.

15 (*a*) C.-M. Che, C. Ho and T.-C. Lau, *J. Chem. Soc., Dalton Trans.*, 1991, 1901–1907; (*b*) W.-C. Cheng, W.-Y. Yu, J. Zhu, K.-K. Cheung, S.-M. Peng, C.-K. Poon and C.-M. Che, *Inorg. Chim. Acta*, 1996, **242**, 105–113; (*c*) W.-Y. Yu, W.-H. Fung, J.-L. Zhu, K.-K. Cheung, K.-K. Ho and C.-M. Che, *J. Chin. Chem. Soc.*, 1999, **46**, 341–349.

16 W.-C. Cheng, W. Y. Yu, K. K. Cheung and C.-M. Che, *J. Chem. Soc., Dalton Trans.*, 1994, 57–62.
17 E. McNeill, Ph.D thesis, Stanford University, 2012.
18 (*a*) I. Garcia-Bosch, A. Company, C. W. Cady, S. Styring, W. R. Browne, X. Ribas and M. Costas, *Angew. Chem., Int. Ed.*, 2011, **50**, 5647–5652; (*b*) L. Gomez, I. Garcia-Bosch, A. Company, J. Benet-Buchholz, A. Polo, X. Sala, X. Ribas and M. Costas, *Angew. Chem., Int. Ed.*, 2009, **48**, 5720–5723.
19 K. Wieghardt, P. Chaudhuri, B. Nuber and J. Weiss, *Inorg. Chem.*, 1982, **21**, 3086–3090.
20 P. Neubold, B. S. P. C. Della Vedova, K. Wieghardt, B. Nuber and J. Weiss, *Inorg. Chem.*, 1990, **29**, 3355–3363.